

Conductance via Multi orbital Kondo Effect in Single Quantum Dot

Rui Sakano and Norio Kawakami
*Department of Applied Physics, Osaka University,
 Suita, Osaka 565-0871, Japan*

(Dated: August 30, 2018)

We study the Kondo effect in a single quantum dot system with two or three orbitals by using the Bethe-ansatz exact solution at zero temperature and the non-crossing approximation at finite temperatures. For the two-orbital Kondo effect, the conductance is shown to be constant at absolute zero in any magnetic fields, but decrease monotonically with increasing fields at finite temperatures. In the case with more orbitals, the conductance increases at absolute zero, while it features a maximum structure as a function of the magnetic field at finite temperatures. We discuss how these characteristic transport properties come from the multi orbital Kondo effect in magnetic fields.

PACS numbers: 73.63.Kv, 73.23.-b, 71.27.+a, 75.30.Mb

I. INTRODUCTION

The Kondo effect is a typical electron correlation problem, which was originally discovered in dilute magnetic alloys as a resistance minimum phenomenon [1, 2]. Although the essence of the Kondo effect was already clarified, it is quite interesting to systematically study the Kondo effect in artificial systems. Recently, the Kondo effect observed in quantum dot systems, which have rich tunable parameters [3, 4], has attracted considerable attention [5, 6, 7]. This has stimulated intensive investigations on electron correlations. Indeed, a lot of the work have been done both theoretically and experimentally.

Among intensive studies, the Kondo effect due to the orbital degrees of freedom is of particular interest, where effective orbitals are given by a highly symmetric shape of the dot, multiply coupled quantum dots, etc [8, 9, 10, 11, 12, 13, 14]. In such systems, not only the ordinary spin Kondo effect [15, 16] but also the orbital Kondo effect due to the interplay between orbital and spin degrees of freedom occurs; the Kondo effect in multiple-dot systems [17, 18, 19, 20, 21, 22, 23, 24, 25, 26], the singlet-triplet Kondo effect [27, 28, 29, 30], and the SU(4) Kondo effect in single-dot systems [31, 32, 33, 34, 35].

In this paper, we focus on the Kondo effect in a single-dot system with multiple orbitals, and explore characteristic transport properties at zero and finite temperatures. To this end, we use the Bethe-ansatz exact solution of the impurity Anderson model and the non-crossing approximation (NCA). To be specific, we deal with a quantum dot system with two or three orbitals as a typical example of the multi-orbital Kondo effect.

Experimentally, the two-orbital Kondo effect (SU(4) Kondo effect) in single-dot systems has already been observed in transport properties, where the conductance shows similar field-dependence to the usual SU(2) spin Kondo effect: in both cases the conductance is monotonically suppressed in the presence of magnetic fields[31, 34]. One of the main purposes of the present paper is to demonstrate that although the field-dependent conductance shows analogous behavior, its origin is different

from each other: the decrease of the conductance in the two-orbital case is due to the decrease of the effective Kondo temperature, in contrast to the ordinary SU(2) Kondo effect. Moreover, we show that in three- or more-orbital cases, the conductance even features a maximum structure in magnetic fields, which is not expected in the ordinary spin Kondo effect.

This paper is organized as follows. In Sec. II, we introduce a generalized impurity Anderson model for our multi-orbital quantum dot system, and outline how to treat transport properties by means of the Bethe-ansatz exact solution at absolute zero and the NCA method at finite temperatures. We investigate the two-orbital Kondo effect in Sec. III, and then move to the case with more orbitals in Sec. IV by taking the three-orbital Kondo effect as an example. We discuss characteristic magnetic-field dependence of the conductance due to orbital effects at zero and finite temperatures. A brief summary is given in Sec. V, where the multi-orbital Kondo effects are compared with the ordinary single-orbital spin Kondo effect.

II. MODEL AND METHOD

A. Multi orbital quantum dot

Let us consider a single quantum dot system with N -degenerate orbitals in equilibrium state. As shown in Fig. 1, we assume that each energy-level splitting between the orbitals is Δ_{orb} in the presence of magnetic field and the Zeeman splitting is much smaller than it, so that we can ignore the Zeeman effect: the degenerate levels are split into N spin doublets. The energy level of each orbital state is specified as

$$\varepsilon_{\sigma l} = \varepsilon_c + l\Delta_{orb} \quad (1)$$

$$(l = -\frac{N-1}{2}, -\frac{N-3}{2}, \dots, \frac{N-1}{2})$$

where ε_c denotes the centre of the energy levels and $l(\sigma)$ represents orbital(spin) index.

This type of orbital splitting has been experimentally realized as Fock-Darwin states in vertical quantum dot systems [8, 36, 37] or clockwise & counter-clockwise states in carbon nanotube quantum dot systems [34], where the orbital splittings are proportional to the magnitude of magnetic fields.

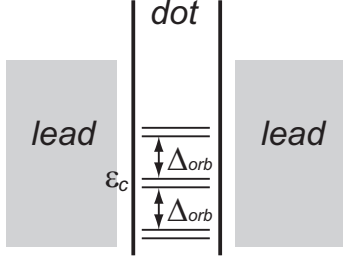


FIG. 1: Energy-level scheme of a single quantum dot with three orbitals coupled to two leads.

B. Bethe-ansatz exact solution

We model the above quantum dot system by assuming that the Coulomb repulsion U between electrons is sufficiently strong at the quantum dot, so that we effectively put $U \rightarrow \infty$. We focus on the N -degenerate orbital states in the quantum dot, which are assumed to hybridize with the corresponding conduction channels in the leads for simplicity. In these assumptions, our system can be described by an $SU(N)$ multi-orbital extension of the impurity Anderson model in the strong correlation limit ($U \rightarrow \infty$). The Hamiltonian reads

$$H = H_0 + H_I, \quad (2)$$

$$H_0 = \sum_{\sigma, l} \varepsilon_{\sigma l} |\sigma l\rangle \langle \sigma l| + \sum_{k \sigma l} \varepsilon_k c_{k \sigma l}^\dagger c_{k \sigma l}, \quad (3)$$

$$H_I = \sum_{k \sigma l} (V_k |\sigma l\rangle \langle 0| c_{k \sigma l} + h.c.), \quad (4)$$

where $c_{k \sigma l}^\dagger (c_{k \sigma l})$ creates (annihilates) a conduction electron with wavenumber k , spin $\sigma (= \pm 1/2)$ and orbital l . An electron state at the dot is expressed as $|\sigma l\rangle$, which is supplemented by the unoccupied state $|0\rangle$.

In spite of its simple appearance, the Hamiltonian (4) is difficult to treat generally because of strong correlations coming from the $U \rightarrow \infty$ condition. Fortunately, this model was extensively studied two decades ago in the context of electron correlations for Ce and Yb rare-earth impurity systems. In particular, the exact solution of the model was obtained by the Bethe ansatz method under the condition that the density of states for electrons in the leads is constant (wide-band limit) [38]. This solution enables us to exactly compute the static quantities, but not transport quantities in a direct way. However, by combining the Landauer formula and the Friedel sum

rule, we can evaluate the zero-bias conductance in the Kondo regime at absolute zero [39, 40],

$$G = \frac{2e^2}{h} \sum_l \sin^2(\pi n_{\sigma l}), \quad (5)$$

where the occupation number of the electron $n_{\sigma l}$ is given by the Bethe-ansatz solution.

C. NCA method

The above technique to calculate the conductance by the exact solution cannot be applied to the finite-temperature case. Therefore, we complementarily make use of the NCA for the analysis at finite temperatures [2, 41]. The NCA is a self-consistent perturbation theory, which summarizes a specific series of expansions in the hybridization V . This method is known to give physically sensible results at temperatures around or higher than the Kondo temperature. In fact, it was successfully applied to the Ce and Yb impurity problem mentioned above, for which orbital degrees of freedom play an important role [42, 43, 44, 45]. Therefore, by combining the exact results at zero temperature with the NCA results at finite temperatures, we can deduce correct behavior of the conductance for the model (4).

The NCA basic equations can be obtained in terms of coupled equations for two types of self-energies $\Sigma_0(z)$ and $\Sigma_{\sigma l}(z)$ of the resolvents $R_\alpha(z) = 1/(z - \varepsilon_\alpha - \Sigma_\alpha(z))$,

$$\Sigma_0(z) = \frac{2\Gamma}{\pi} \sum_l \int_D^D d\varepsilon \frac{f(\varepsilon)}{z - \varepsilon_{\sigma l} + \varepsilon - \Sigma_{\sigma l}(z + \varepsilon)}, \quad (6)$$

$$\Sigma_{\sigma l}(z) = \frac{\Gamma}{\pi} \int_D^D d\varepsilon \frac{1 - f(\varepsilon)}{z - \varepsilon_0 + \varepsilon - \Sigma_0(z + \varepsilon)}, \quad (7)$$

for the flat conduction band of width $2D$. At finite temperatures, the conductance is given as [46],

$$G = \frac{2e^2}{h} \Gamma \sum_l \int d\varepsilon \left(-\frac{df(\varepsilon)}{d\varepsilon} \right) A_{\sigma l}(\varepsilon), \quad (8)$$

where $f(\varepsilon)$ is the Fermi distribution function and $A_{\sigma l}(\varepsilon)$ is the one-particle spectral function including the effect of the above self-energies.

III. TWO-ORBITAL KONDO EFFECT

We begin with a quantum dot system with two orbitals ($N = 2$), where it is assumed that the orbital degeneracy is lifted by a splitting Δ_{orb} while the spin degeneracy remains in the presence of magnetic field. As mentioned above, the two-orbital Kondo effect, often referred to as the doublet-doublet or $SU(4)$ Kondo effect, has been experimentally observed in vertical dot systems and carbon nanotube dot systems [31, 34]. We will be mainly concerned with the Kondo regime, where the characteristic energy scale is given by the Kondo temperature $T_K^{SU(4)}$.

A. Exact results at absolute zero

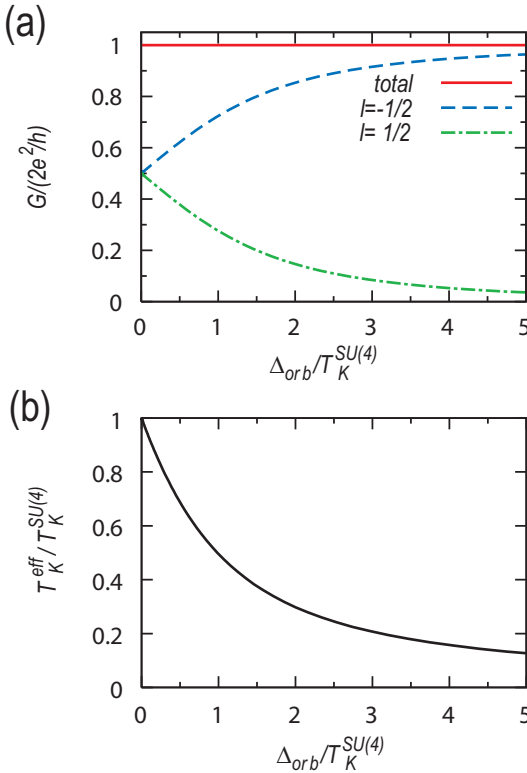


FIG. 2: (a) Zero-temperature conductance calculated by the exact solution as a function of the energy splitting for the SU(4) Anderson model in the Kondo regime. The total conductance is constant, although the contributions from two orbitals are changed monotonically. (b) The effective Kondo temperature T_K^{eff} .

It is known that the conductance for the SU(4) case ($\Delta_{orb} = 0$) and the SU(2) case ($\Delta_{orb} = \infty$) is both given by $2e^2/h$ at absolute zero. However, the conductance in the intermediate coupling region ($\Delta_{orb} = \text{finite}$) has not been discussed so far. The calculated conductance for each orbital is shown in Fig. 2(a), which changes smoothly around the Kondo temperature $T_K^{SU(4)}$. An important point is that the total conductance is always $2e^2/h$, which is independent of magnetic fields. In fact, by putting the occupation number $n_{\sigma,\pm 1/2} = 1/4 \mp \delta n(\Delta_{orb})$ into Eq. (5), we can readily derive the constant conductance in the presence of magnetic fields. This result is characteristic of the SU(4) case, which is consistent with those deduced for the double-dot system with a special setup [18].

It should be noted here that there is another important effect due to magnetic fields: the effective Kondo temperature changes with magnetic fields. The effective Kondo temperature, which is defined by the inverse of the spin susceptibility for the lowest doublet, gives the width of the effective Kondo resonance in the presence

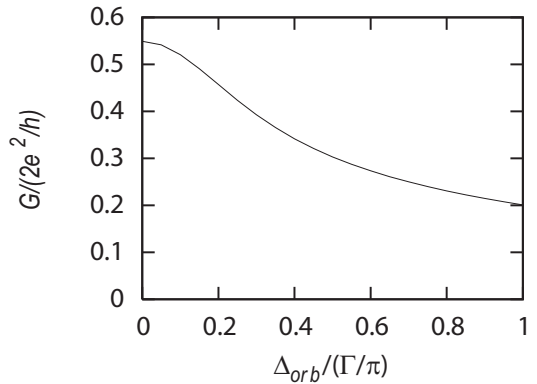


FIG. 3: Finite-temperature conductance computed by the NCA as a function of the energy splitting for the SU(4) model in the Kondo regime: $k_B T = 0.1\Gamma/\pi$ where Γ is the bare resonance width. The energy level of the dot is $\epsilon_c = -20\Gamma/\pi$, which gives the SU(4) Kondo temperature $T_K^{SU(4)} \sim 0.1\Gamma$.

of the orbital splitting. As seen in Fig. 2(b), it monotonically decreases, and is inversely proportional to the orbital splitting in the asymptotic region: $T_K^{eff} \sim 1/\Delta_{orb}$ [22, 33, 47, 48].

B. Analysis at finite temperatures

It is remarkable that the conductance does not depend on magnetic fields at absolute zero, however, we should recall that the conductance is experimentally observed at finite temperatures. Since the Kondo temperature provides the characteristic energy scale of the system, the decrease of the effective Kondo temperature should have a tendency to suppress the Kondo effect at a given finite temperature. Therefore, we naturally expect from the zero-temperature analysis that the conductance monotonically decreases with increasing magnetic fields at a finite temperature. This can be confirmed by the NCA numerical calculations at finite temperatures. The results are shown in Fig. 3, from which we indeed see the monotonic decrease of the conductance. The obtained results qualitatively agree with the experimental observation of the SU(4) Kondo effect in the quantum dot systems [31, 34]. We wish to emphasize again that the magnetic-field dependence found here is different from that discussed so far for the ordinary spin Kondo effect without orbitals: the decrease of the conductance is caused by the decrease of the Kondo temperature in our scenario for the SU(4) case.

IV. THREE-ORBITAL KONDO EFFECT

In the previous section, we have considered the conductance for the two-orbital Kondo effect. We now generalize our treatment to the multiorbital cases with more

than two orbitals. In contrast to the two-orbital case, where the conductance at finite temperatures shows behavior similar to the usual spin Kondo effect, we will see that the conductance for three- or more- orbital systems shows qualitatively different behavior in the magnetic-field dependence. This provides us with an efficient way to characterize the multi-orbital Kondo effect experimentally. Here, we discuss the characteristic transport properties by taking the three-orbital Kondo effect ($N = 3$) as an example.

A. Exact results at absolute zero

Exploiting the Bethe-ansatz exact solution and the Landauer formula, we calculate the conductance at $T = 0$ for the single-dot system with three orbitals in the Kondo regime. We note that Schlottmann studied a similar model for Ce-impurity systems in a crystalline field to discuss its magnetic properties [49]. The conductance

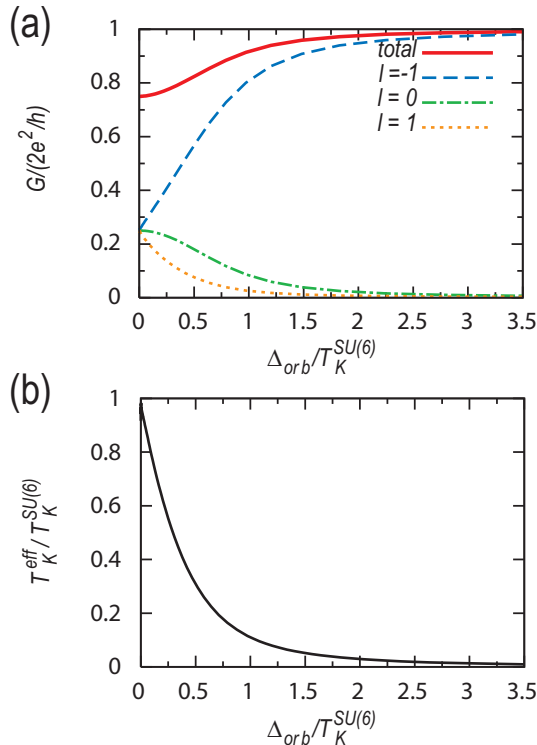


FIG. 4: (a) Conductance calculated by the exact solution at absolute zero as a function of the energy splitting Δ_{orb} . Each line represents the total or the contributions from each orbital state. The system is in Kondo regime: the total number of the electrons in the quantum dot is $n_d = 1$. (b) The effective Kondo temperature $T_K^{SU(6)}$.

computed by the exact solution is shown as a function of the energy splitting in Fig. 4. It is seen that the total conductance at zero temperature monotonically increases from $3e^2/2h$ (SU(6) case) with the increase of

energy splitting (or magnetic field), and approaches the value of $2e^2/h$ for large splittings (SU(2) case). It is noteworthy that the conductance is enhanced by the magnetic field in contrast to the ordinary spin Kondo effect without orbital degrees of freedom, for which the conductance is simply suppressed by the magnetic field. In more general cases with N orbitals, the conductance increases from $(2Ne^2/h) \sin^2(\pi/(2N))$ to $2e^2/h$ with the increase of the magnetic field since the electron number of the lowest-orbital state changes from $1/(2N)$ (zero field) to $1/2$ (large fields). This analysis at zero temperature naturally leads us to predict the following behavior at finite temperatures. Since the magnetic field decreases the effective Kondo temperature, there appears the competition between enhancement and suppression of the Kondo effect at finite temperatures. As a consequence, a maximum structure should appear in the conductance as a function of the magnetic field in general cases with more than two orbitals. This unique feature distinguishes the three- or more-orbital Kondo effect from the two-orbital Kondo effect.

B. Analysis at finite temperatures

Here, we wish to confirm the conductance maximum at finite temperatures predicted from the zero-temperature analysis. The conductance for the three-orbital Kondo effect computed by the NCA at finite temperatures is shown in Fig. 5. At low temperatures, the predicted maximum structure indeed emerges in the conductance as a function of the energy splitting. It is seen that the height of the maximum grows and its position gradually shifts toward the region with larger splitting Δ_{orb} as the temperature decreases. The shift reflects the fact that the suppression of the Kondo effect due to the decrease of the Kondo temperature becomes somewhat weaker at lower temperatures.

To see how the conductance maximum structure emerges for the three-orbital Kondo effect, we show the one-particle spectral density $A(\omega)$ computed at $k_B T = 0.083\Gamma/\pi$ in Fig. 6. For the case of $\Delta_{orb} = 0$ (three degenerate orbitals), there is a single SU(6) Kondo peak, while for $\Delta_{orb} = 0.5\Gamma/\pi$, it splits into three peaks. For $\Delta_{orb} = 2.0\Gamma/\pi$, we can see that the SU(2) Kondo peak is developed around the Fermi level $\omega = 0$, for which only the lowest energy level ($l = -1$) is relevant. Note that further increase of the energy splitting should have a tendency to suppress the above SU(2) Kondo effect at a given temperature because of the decrease of the effective Kondo temperature. The enlarged picture of the spectral density around the Fermi level is shown in Fig. 6(b), which determines the linear conductance at low temperatures. It is seen that the spectral weight around the Fermi level once increases and then decreases with increasing energy splitting, which gives rise to the maximum structure in the conductance.

TABLE I: Comparison of the conductance among different Kondo effects in the presence of magnetic field at zero and finite temperatures.

temperature	spin Kondo effect	two-orbital Kondo effect	three- or more-orbital Kondo effect
$T = 0$	decrease	constant $2e^2/h$	increase up to $2e^2/h$
$T \neq 0$	decrease	decrease	maximum

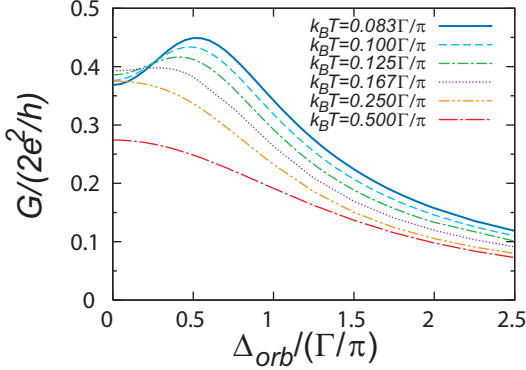


FIG. 5: Conductance for the three-orbital Kondo effect computed by the NCA calculation at different temperatures as a function of the orbital splitting Δ_{orb} . The parameter is $\varepsilon_c = -25\Gamma/\pi$, which gives $T_K^{SU(6)} \sim 0.2\Gamma$. At low temperatures, the predicted maximum structure appears. Note that for $\Delta_{orb} = 0$ and $k_B T = 0.083\Gamma/\pi$, the total number of the electrons in the quantum dot is $n_d \sim 0.82$.

V. SUMMARY

We have discussed transport properties via the multi-orbital Kondo effect in a single quantum dot system by using the Bethe-ansatz exact solution at zero temperature and the NCA at finite temperatures. It has been shown that the orbital Kondo effect gives rise to some remarkable transport properties, which are different from the ordinary spin Kondo effect. The results are summarized in TABLE I in comparison with the usual SU(2) spin Kondo effect.

For the two-orbital SU(4) Kondo effect, it has been found that the conductance at absolute zero is constant ($2e^2/h$) irrespective of the strength of magnetic fields. However, the effective Kondo temperature, which gives the energy scale at low-temperatures, decreases monotonically. Therefore, if the conductance is observed at finite temperatures, it decreases with the increase of the magnetic field, in accordance with the recent experimental results for the conductance in the vertical quantum and the carbon nanotube quantum dot system [31, 34]. We stress again that although the magnetic-field dependence at finite temperatures seems similar to the conventional SU(2) spin Kondo effect at first glance, the mechanism is different: the decrease of the conductance in the two-orbital SU(4) Kondo effect is due to the decrease of the effective Kondo temperature. This fact should be properly taken into account for the detailed analysis of the

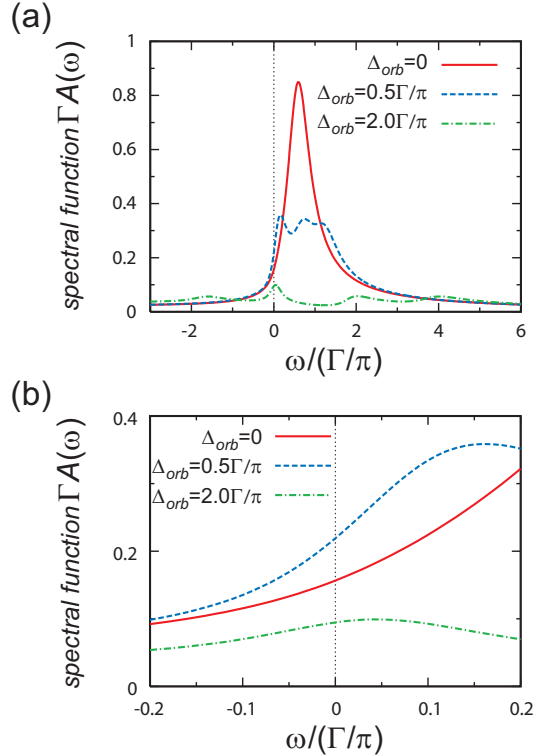


FIG. 6: (a) NCA results for the total spectral density $A(\omega)$ for different orbital splittings at $k_B T = 0.083\Gamma/\pi$. (b) Zoom of $A(\omega)$ around the Fermi level of electrons in the leads $\omega = 0$. The bare energy level is $\varepsilon_c = -25\Gamma/\pi$.

field-dependent conductance due to the SU(4) Kondo effect.

In the three-orbital or more-orbital cases, the conductance at absolute zero increases in magnetic fields, and is then saturated at the value of $2e^2/h$. In this case also, the effective Kondo temperature decreases as the field increases, so that the conductance features a maximum structure at finite temperatures. Such unusual behavior in the conductance may be observed experimentally in vertical quantum dot systems by tuning multi-orbital degenerate states systematically [50].

In this paper, we have considered a simplified model for the quantum dot with multiple orbitals: e.g. the tunneling matrix elements between the leads and the dot are assumed to be constant and independent of orbitals. We believe that in spite of such simplifications the present model captures essential properties inherent in the multi-orbital Kondo effect at least qualitatively. It remains an

interesting problem to improve our model by incorporating the detailed structure of the quantum dot parameters, which is now under consideration.

Acknowledgments

We would like to express our sincere thanks to M. Eto and S. Amaha for valuable discussions. R.S. also thanks

H. Yonehara for advices on computer programming, and T. Ohashi and T. Kita for discussions.

[1] J. Kondo, *Prog. Theor. Phys.* **32**, 37 (1964).

[2] A. C. Hewson, *The Kondo Problem to Heavy Fermions* (Cambridge University Press, Cambridge, 1997).

[3] L. P. Kouwenhoven, D. G. Austing, and S. Tarucha, *Rep. Prog. Phys.* **64**, 701 (2001).

[4] S. M. Reimann and M. Manninen, *Rev. Mod. Phys.* **74**, 1283 (2002).

[5] D. Goldhaber-Gordon, J. Góres and M. A. Kastner, *Nature (London)* **391**, 156 (1998); *Phys. Rev. Lett.* **81**, 5225 (1998).

[6] S. M. Cronenwett, T. H. Oosterkamp, and L. P. Kouwenhoven, *Science* **281**, 540 (1998).

[7] J. Schmid, J. Weis, K. Eberl, and K. v. Klitzing, *Physica B* **256**, 182 (1988).

[8] S. Tarucha, D. G. Austing, T. Honda, R. J. van der Hage and L. P. Kouwenhoven, *Phys. Rev. Lett.* **77**, 3613 (1996).

[9] S. Moriyama, T. Fuse, M. Suzuki, Y. Aoyagi, and K. Ishibashi, *Phys. Rev. Lett.* **94**, 186806 (2005).

[10] P. Jarillo-Herrero, J. Kong, H. S. J. van der Zant, C. Dekker, L. P. Kouwenhoven, and S. De Franceschi, *Phys. Rev. Lett.* **94**, 156802 (2005).

[11] S. Bellucci and P. Onorato, *Phys. Rev. B* **71**, 075418 (2005).

[12] D. H. Cobden and J. Nygard, *Phys. Rev. Lett.* **89**, 046803 (2002).

[13] Y. Asano, *Phys. Rev. B* **58**, 1414 (1998).

[14] S. Park and S.-R. E. Yang, *Phys. Rev. B* **72**, 125410 (2005).

[15] T. K. Ng and P. A. Lee, *Phys. Rev. Lett.* **61**, 1767 (1988).

[16] L.I. Glazman and M. É. Raikh, *JETP Lett.* **47**, 452 (1988).

[17] U. Wilhelm, and J. Weis, *Physica E* **6**, 668 (2000).

[18] L. Borda, G. Zaránd, W. Hofstetter, B. I. Halperin, and J. von Delft, *Phys. Rev. Lett.* **90**, 26602 (2003).

[19] Mei-Rong Li and Karyn Le Hur, *Phys. Rev. Lett.* **93**, 176802 (2004).

[20] A. W. Holleitner, A. Chudnovskiy, D. Pfannkuche, K. Eberl, and R. H. Blick *Phys. Rev. B* **70**, 075204 (2004).

[21] Martin R. Galpin, David E. Logan, and H. R. Krishnamurthy, *Phys. Rev. Lett.* **94**, 186406 (2005).

[22] R. Sakano and N. Kawakami, *Phys. Rev. B* **72**, 085303 (2005).

[23] R. López, D. Sánchez, M. Lee, M.-S. Choi, P. Simon, and K. Le Hur, *Phys. Rev. B* **71**, 115312 (2005).

[24] A. L. Chudnovskiy, e-print, cond-mat/0502282 (2005).

[25] T. Kuzmenko, K. Kikoin, and Y. Avishai, e-print, cond-mat/0507488 (2005).

[26] S. Lipinski and D. Krychowski, *Phys. stat. sol. (b)* **246** (2006) in press.

[27] S. Sasaki, S. De Franceschi, J. M. Elzerman, W. G. van der Wiel, M. Eto, S. Tarucha and L. P. Kouwenhoven, *Nature*, **405**, 764 (2000).

[28] K. Kikoin and Y. Avishai, *Phys. Rev. Lett.* **86**, 2090 (2001).

[29] M. Pustilnik and L. I. Glazman, *Phys. Rev. B* **64** 045328 (2001).

[30] M. Eto and Y. V. Nazarov, *Phys. Rev. B* **64**, 085322 (2001).

[31] S. Sasaki, S. Amaha, N. Asakawa, M. Eto, and S. Tarucha, *Phys. Rev. Lett.* **93**, 017205 (2004).

[32] A. K. Zhuravlev, V. Yu. Irkhin, M. I. Katsnelson, and A. I. Lichtenstein, *Phys. Rev. Lett.* **93**, 236403 (2004).

[33] M. Eto, *J. Phys. Soc. Jpn.* **74**, 95 (2004).

[34] P. Jarillo-Herrero, J. Kong, H. S.J. van der Zant, C. Dekker, L. P. Kouwenhoven, and S. De Franceschi, *Nature* **434**, 484 (2005).

[35] M.-S. Choi, R. Lópetz, and R. Aguado, *Phys. Rev. Lett.* **95**, 067204 (2005).

[36] V. Fock, *Z. Phys.* **47**, 446 (1928); C. G. Darwin, *Proc. Cambridge Philos. Soc.* **27**, 86 (1930).

[37] Y. Tokura, S. Sasaki, D. G. Austing, and S. Tarucha, *Physica B*, **298**, 260 (2001).

[38] P. Schlottmann, *Phys. Rev. Lett.* **50**, 1697 (1983); N. Kawakami, and A. Okiji, *J. Phys. Soc. Jpn.* **54**, 685 (1985).

[39] A. Kawabata, *J. Phys. Soc. Jpn.* **60**, 3222 (1991).

[40] Y. Meir and N. S. Wingreen, *Phys. Rev. Lett.* **68**, 2512 (1992).

[41] N. E. Bickers, *Rev. Mod. Phys.* **59**, 845 (1987).

[42] Y. Kuramoto, *Z. Phys. B* **53**, 37 (1980).

[43] F. C. Zhang and T. K. Lee, *Phys. Rev. B* **28**, 33 (1983).

[44] P. Coleman, *Phys. Rev. B* **28** 5255 (1983).

[45] S. Maekawa, S. Takahashi, S. Kashiba, and M. Tachiki, *J. Phys. Soc. Jpn.* **54**, 1955 (1985).

[46] M. H. Hettler, J. Kroha and S. Hershfield, *Phys. Rev. B* **58**, 5649 (1998).

[47] P. Schlottmann, *Phys. Rev. B* **30**, 1454 (1984).

[48] K. Yamada, K. Yoshida, and K. Hanzawa, *Prog. Theor. Phys.* **71**, 450 (1984).

[49] P. Schlottmann, *J. Mag. Mag. Mater.* **52**, 211 (1985).

[50] private communication, S. Amaha and S. Tarucha.